AFOSR-TR-95

0593

REPORT DOCUMENTATION PAGE

FINAL/01 MAY 94 TO 30 APR 95

PHASE CONTROL OF A MICROSTRIP PATCH ANTENNA

2304/IS
F49620-94-1-0212

MICHAEL H. THURSBY, Ph.D.

AUTONOMYS SYSTEMS LABORATORY
FLORIDA INSTITUTE OF TECHNOLOGY
150 W. UNIVERSITY BLVD.
MELBOURNE, FLORIDA 32901

AFOSR/NM
110 DUNCAN AVE, SUTE B115
BOLLING AFB DC 20332-0001

F49620-94-1-0212

11. SUPPLEMENTARY NOTES

APPROVED FOR PUBLIC RELEASE: DISTRIBUTION IS UNLIMITED

Under this Air Force grant we have begun the investigation into the ability of the embedded impedance elements to control the far field phase of an individual element with the anticipation that this element can be incorporated into an array and used in a manner of similar to phase steered array using external phase shifters. The advantage of this approach is that the phase shifting devices are embedded in the antenna and are extremely simple in composition. This eliminates several connections to the antenna elements as well as the need for external devices. The potential payoffs include significant weight reduction and increased reliability with fewer mechanical connections. The total reliability, maintainability, and efficiency of the elements and the array will be increased significantly with this device.

UNCLASSIFIED	UNCLASSIFIED	UNCLASSIFIED	SAR(SAME AS REPORT)

Phase Control of a Microstrip Patch Antenna

A final report for the work done under
A.F. Grant #F469620-94-0212
from June, 1994 - August, 1995

Submitted August 9, 1995

By
Michael H. Thursby, Ph.D.
Tel. (407) 768-8000 x6160
E-mail mthursby@zach.fit.edu

Autonomys Systems Laboratory
Florida Institute of Technology
150 W. University Blvd.
Melbourne, Florida 32901

Table of Contents

Introduction	1
Microstrip patch antenna history	2
Previous work on the phase controlled microstrip patch antenna	3
Theoretical results	4
Experimental results	12
Conclusions and future research	17
References	18

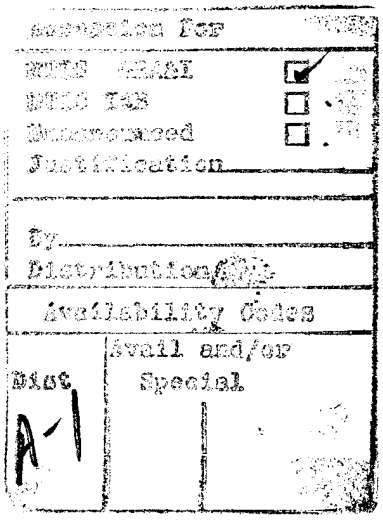

Introduction

Microstrip patch antennas (MPA) have provided effective solutions to antenna problems for many years. The advantages of the microstrip patch antenna are low cost, low profile, conformability, and ease of manufacture. The drawbacks, however, include narrow bandwidth, low power capacity, and the excitation of surface waves. A number of improvements in the characteristics of the microstrip patch antenna have been described by several authors over the past decade. The microstrip patch antenna is considered a standard radiating element in the design of monolithic phased arrays for applications requiring light weight and small element size. Such designs require the use of conventional phase shifting elements. With this, one must consider insertion loss, switching time, drive power, phase error, physical size, weight, cost, and manufacturing ease. An embedded low-profile phase shifting element would reduce or eliminate the significance of many of these factors in the design cycle.

The purpose of this study was to investigate the feasibility of using embedded impedance elements to control the far field transmission phase of a microstrip patch antenna element. Previous work including Thursby et. al. [17,24] have demonstrated the ability to tune frequency by using embedded impedance elements in the microstrip patch antenna. Under this Air Force grant we have begun the investigation into the ability of the embedded impedance elements to control the far field phase of an individual element with the anticipation that this element can be incorporated into an array and used in a manner similar to phase steered arrays using external phase shifters. The advantage of this approach is that the phase shifting devices are embedded in the antenna and are extremely simple in composition. This eliminates several connections to the antenna elements as well as the need for external devices. The potential payoffs include significant weight reduction and increased reliability with fewer mechanical connections. The total reliability, maintainability, and efficiency of the elements and the array will be increased significantly with this device.

Microstrip Patch Antenna History

The microstrip antenna concept can be traced back to the work done by D. D. Greig et al. in 1952 [1] and G. A. Deschamps in 1953 [2]. However, it wasn't to attract attention until the need for low-profile antennas arose in the early 1970s [27] which can be found in [3,4] for circular resonant microstrip, and [5] for L-band rectangular microstrip antennas. The earlier theoretical model for microstrip patch antenna was a simple transmission line model introduced by R. E. Munson in 1974 [6] and extended by A. G. Derneryd in 1976 [7]. This model cannot be applied to geometries other than rectangular. A transmission line model incorporating short circuit loads was described by Schaubert et al. in 1981 [8]. However, the ability to accurately predict the input impedance of a loaded element is limited in this model [12]. A simple cavity model was introduced by Y.T. Lo et al. in 1979 [9]. This model was well suited for predicting impedance loci, radiation patterns, and resonant frequencies for the unloaded element. An improved cavity model introduced by W. F. Richards et al. in 1981 [10] considers all losses including radiated loss, surface-wave loss, and copper wall loss as an effective loss tangent. This model enhanced the accuracy of results as well as the computational efficiency [10]. A reactively loaded cavity model introduced by W. F. Richards et al. in 1984 [11,12] provides a reasonably accurate reactive load model for the loaded element. A multiport network model (MNM) introduced by K. C. Gupta in 1987 [14] replaces the fields outside the patch including the radiation field, the surface-wave fields, and the fringing fields at the edges with equivalent edge admittance networks (EAN) connected to edges of the patch [15]. A mutual coupling network (MCN) was used to extend the model to incorporate the effect of mutual coupling between the two radiating edges in 1989 [16]. In this MNM, the fields underneath the patch are similar to those in the cavity model [9,10]. The MNM may be considered as the extension of the cavity model [15]. Therefore, generally speaking, the cavity model is prefered over the transmission line model or the grid wire model. The wire model introduced by P. K. Agrawal in 1977 [13] provides little physical insight into the field structure under the patch [10], and is not suited for adding reactive loads. A varactor diode loaded MPA for frequency agility was proposed by P. Bhartia et al. in 1982 [17]. A frequency agile varactor tuned MPA used in a smart electromagnetic structure and was demonstrated by M. Thursby et al. in 1990 [18]. Equivalent circuit models of the varactor diode were investigated by J. T. Aberle et al. [19]. and R. B. Waterhouse [20] in 1992. A method of moments (MOM) technique was used to provide a Galerkin solution of the electric field integral equation (EFIE) describing the field structure underneath a patch. Applications of this MOM technique can be found in [21,22,23]. The operating frequency of a reactively loaded MPA can be controlled by a neural network processor to adapt to electromagnetically noisy environments. This type of application can be found in [24,25,26].

Previous Work on the Phase Controlled Microstrip Patch Antenna

Year 93-94 A new load structure was implemented as shown in Figure 1. This structure, excluding the varactor, has a series capacitor between the guard ring and the actual ground plane. It was found that this configuration performed similarly to our previous single varactor loaded MPA. However, without this series capacitor between the guard ring and the actual ground plane, it was found that the *impedance phase* increased about 100 degrees over a 0 to 5 volt bias range applied to the varactor without significantly changing the resonant frequency as shown in Figure 2. This led us to study the effect on the *transmission phase* of the antenna.

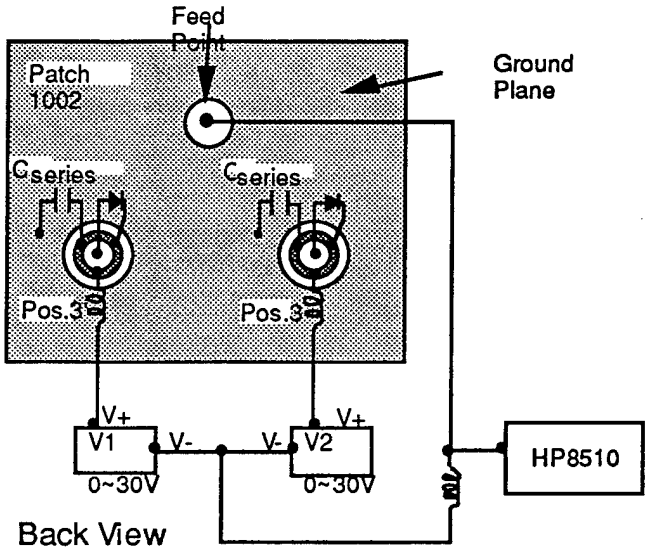

Figure 1. *Guard-ring load configuration*

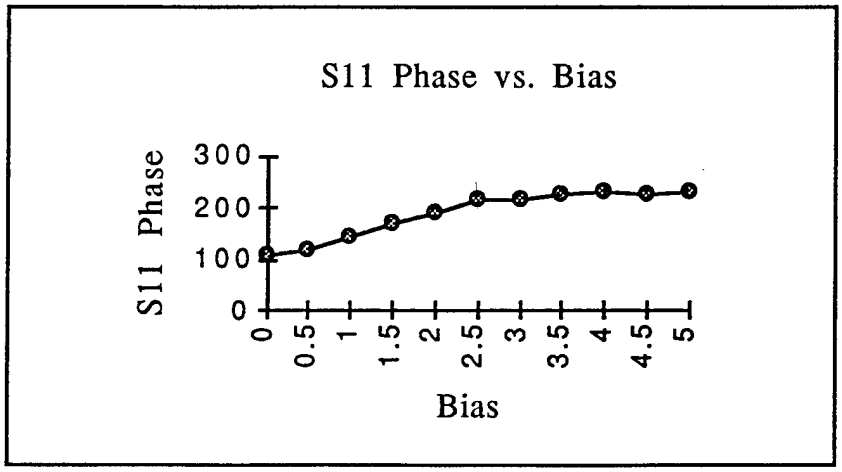

Figure 2. *Impedance phase variation vs. bias voltage*

Theoretical Results

Year 94-95 In this phase of the project, we sought to find a suitable electromagnetic simulation package for our antenna configuration. After an exhaustive survey of the software packages available, we decided to use the IE3D electromagnetic simulation software package from Zeland Software Inc. The IE3D is an integrated full-wave electromagnetic simulation package for the analysis and design of 2-1/2-dimensional microstrip antennas. It uses an integral equation algorithm (Moment Method) to solve for the surface current distribution on an arbitrarily shaped 2-1/2-dimensional printed circuit, and then extracts such circuit parameters as S, Y, and Z parameters as well as lumped element equivalent circuits in SPICE format. The theory behind IE3D is based on solving the electric field integral equation by the moment method which reduces the integral equation to a system of simultaneous linear equations. For example, the electric field integral equation of a conducting wire is given by

$$\frac{1}{j\omega\varepsilon_0}\int_{-L/2}^{L/2} I(z')\left[\frac{\partial^2\psi(z,z')}{\partial z^2}+\beta^2\psi(z,z')\right]dz' = -E_z^i(z)$$

where β is the propagation constant, L is the length of the wire, E_z^i is the incident electric field, $\psi(z,z')$ is the free space Green function.
We can rewrite the above integral equation in the general form

$$\int_{-L/2}^{L/2} I(z')K(z,z')dz' = -E_z^i(z).$$

By applying the moment method, the above integral equation reduces to

$$\sum_{n=1}^{N} Z_{mn} I_n = V_m, \qquad m=1,2,3,...,N$$

where N is the number of segments on the wire, Z_{mn} is the mn^{th} element in the generalized impedance matrix, I_n is the unknown n^{th} element in the current matrix, V_m is m^{th} element in the voltage matrix.
The unknown surface current I can be solved by inverting the above equation:

$$[\, I_n \,] = [Z_{mn}]^{-1}\, [V_m].$$

This represents the desired solution for the current distribution on the surface of the wire. It can be combined with the free space Green function in a superposition integral to solve for the fields radiated by the wire. The IE3D manufacturer has been very cooperative in adding capabilities to IE3D which allowed us to simulate the dual probe loading configuration

which will be described subsequently. Currently we have a package that gives us the ability to predict the near and far field characteristics of the loaded antenna element.

Features of IE3D

- 2-1/2 Dimensional full-wave electromagnetic simulation capability.
- Allows lumped elements to be attached to the microstrip patch antenna.
- Supports a common negative port as well as a ground port. This new feature enabled us to model the dual-probe loading structure.
- Produces steady state surface current data for post-processing.
- Produces both near-field and far-field magnitude and phase data.
- Provides 2 dimensional surface current distribution plot.
- Provides 2 dimensional surface current animation plot.
- Provides 2 dimensional far-field radiation pattern plot.
- Provides 3 dimensional far-field radiation pattern plot.
- Provides 3 dimensional near-field electric field distribution plot.
- User friendly interface on both input and output.
- Unlimited number of substrate layers.
- Arbitrary substrate thickness.
- Complex dielectric permittivity, permeability, and conductivity.
- Complex ground plane permittivity, permeability, and conductivity.
- Unlimited number of ports.
- Unlimited number of unknowns.
- Unlimited number of metallization layers.
- User definable metallic strip loss.
- User definable metallic strip thickness.

To verify the accuracy of the IE3D simulation software, a circular patch antenna with an embedded varactor diode load was modeled. The geometry of this circular patch is described in [19]. A comparison of experimental data with simulation data from the IE3D model showed that IE3D predicted virtually identical results to those presented in the paper. (See Figure 3) With this in mind, we proceeded to model a rectangular patch antenna at a frequency of 2.3 Ghz.

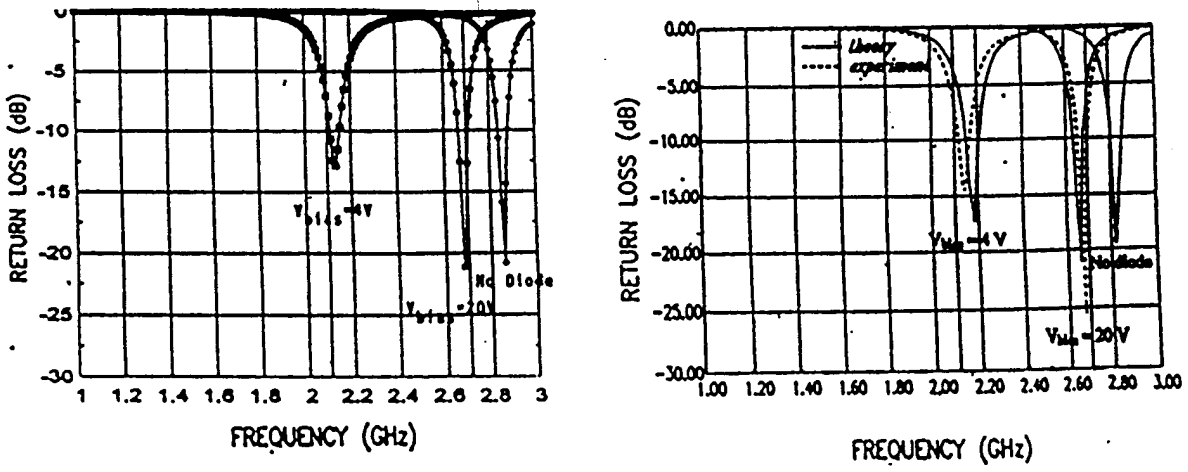

Figure 3. *Comparison of IE3D with published literature*

Theoretical results for single load single probe antenna A side view of the geometry of our varactor loaded rectangular patch antenna is shown in Figure 4. The dielectric constant of the substrate is 2.33. The thickness of the substrate is 16 mils (1mil = 0.001 inch). and the patch dimensions are 1831 mils by 1654 mils. The patch is fed by coaxial cable at x = 911 mils and y = 1403 mils as shown in Figure 5 and is modeled by a vertical strip having a width the same as the inner conductor of the coaxial cable. The thickness of the top copper patch of the antenna is assumed to be infinitely thin, and the ground plane of the patch is infinitely large. The resonant frequency of this patch is 2.3 Ghz, and the steady-state surface current distribution illustrates the dominant TM01 mode of the patch [28]. The position of the load is at x = 351 mils and y = 468 mils. The impedance of the varactor diode was modeled as a complex impedance R+jX where R and X are the resistance and reactance of the load, respectively. In the following simulation, the magnitude and phase of the transmission coefficient S21 in the far field (as depicted in Figure 6 and 7) was calculated in IE3D while the load reactance was allowed to sweep from -97 to 250 ohms. The results of this simulation predicted that between 30 and 40 degrees of S21 transmission phase shift within the -3 dB limits of the forward gain was possible with this loading configuration and position on the patch.

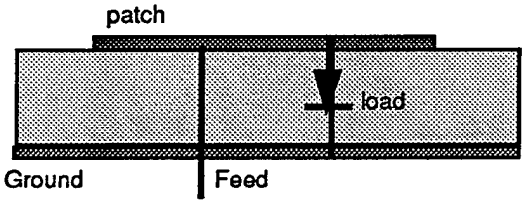

Figure 4. *Side view of the patch antenna with single probe loading scheme*

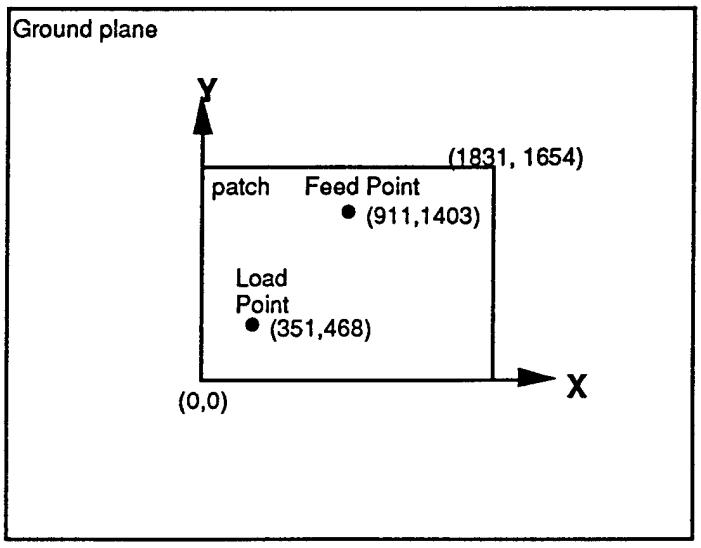

Figure 5. *Top view of the patch antenna with single load single probe loading scheme*

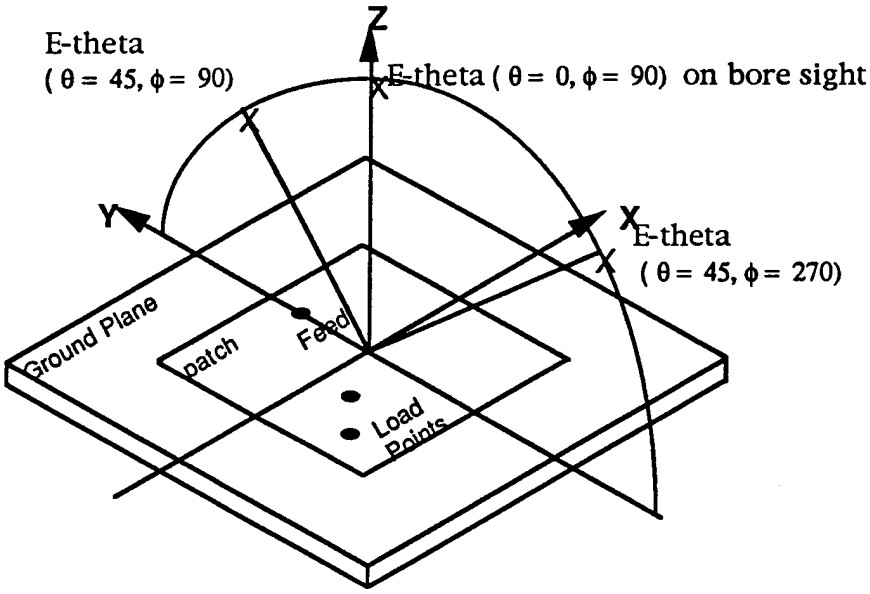

Figure 6. *Orientation of the patch and the far-field E theta*

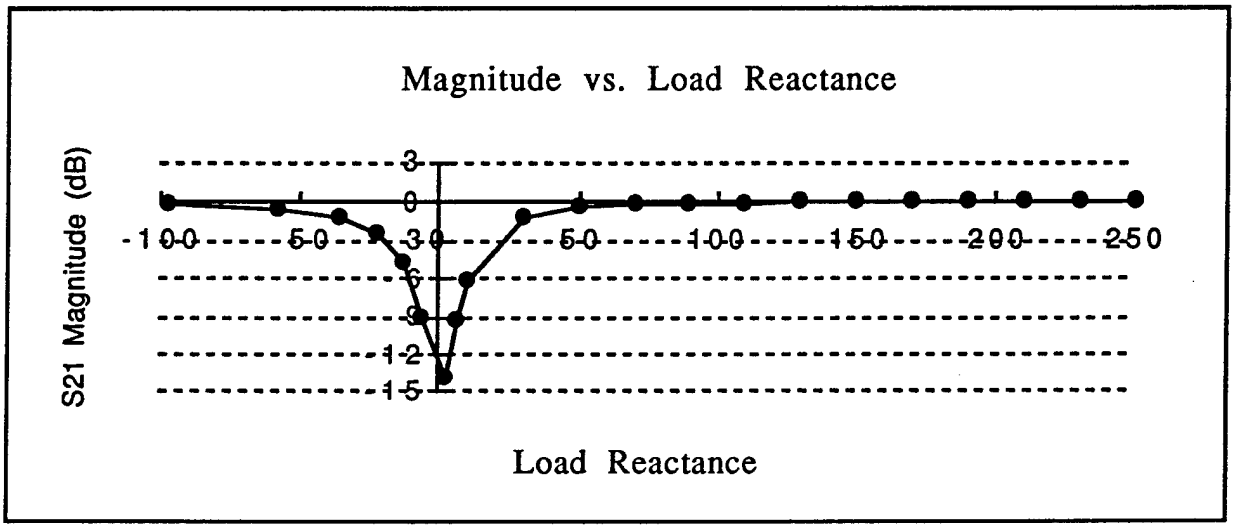

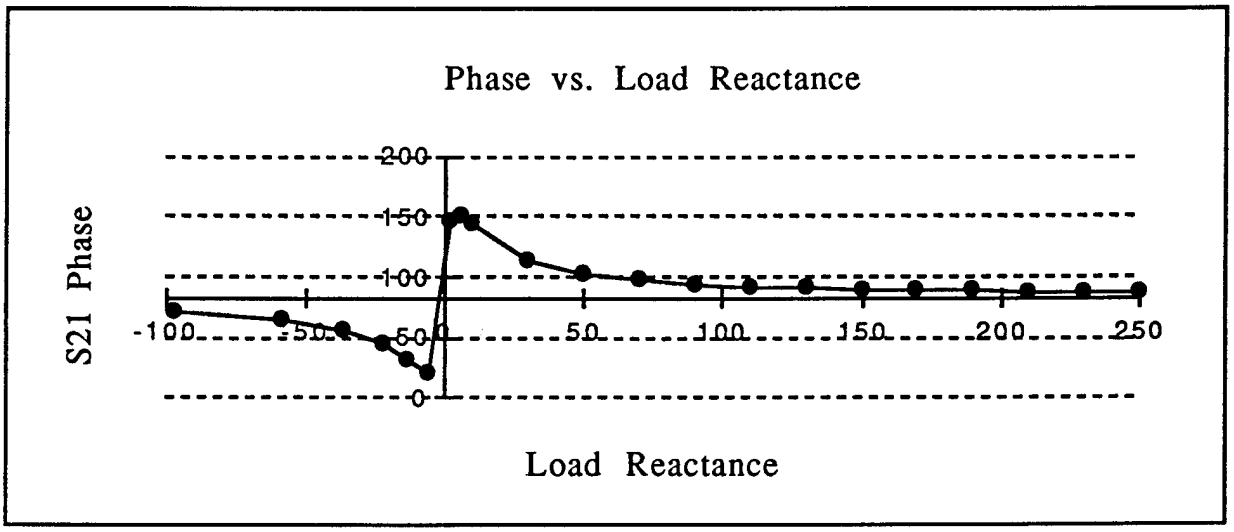

Figure 7. *Magnitude & phase of far-field electric field vs. load reactance*

Theoretical results for the dual probe antenna A second effort to control the far-field transmission phase involved the use of a different loading scheme in which *both* leads of the varactor were attached to the patch through probes. This loading scheme is illustrated in Figure 8 and has been designated as the "*dual probe*" configuration. The previous scheme, designated as the "*single probe*" configuration, is one in which the varactor leads are connected between the patch and the ground plane as shown in Figure 4. The patch antenna described here in Figure 8 is the same as the one described in Figure 4 except for the loading scheme. Four loading configurations were simulated in IE3D. One probe of the dual probe load was fixed at the position A (x = 351 mils and y = 347 mils) as shown in Figure 9. The second probe is moved successively from B to C to D to E. Positions B, C and D are located the same distance (320 mils) from position A and position E is placed at the opposite corner of the square (320 mils x 320 mils) from position A as shown in Figure 9.

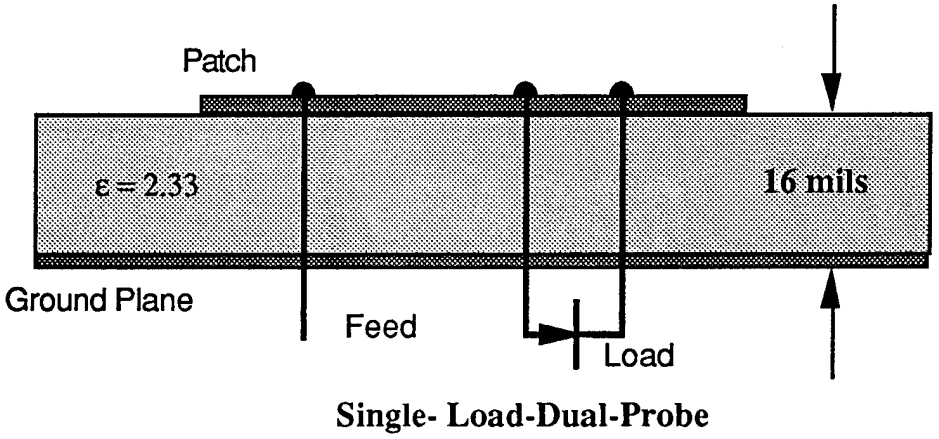

Figure 8. *Schematic representation of dual probe loading scheme.*

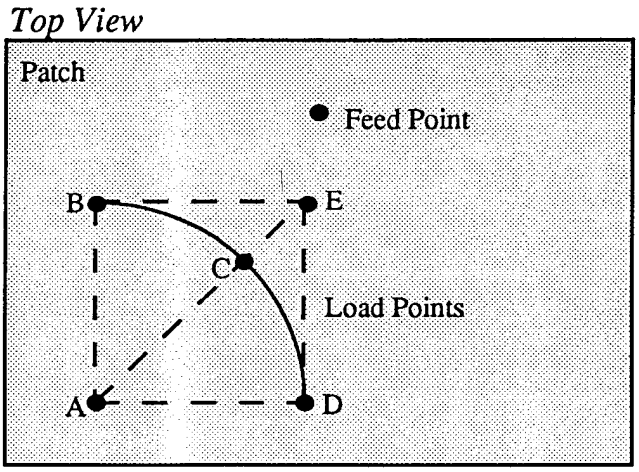

Figure 9. *Top view of dual-probe loading configurations.*

Simulation results and delta phase angle definition The magnitude and phase of the transmission coefficient S21 in the far field (on boresight) were calculated in IE3D while the load reactance was allowed to sweep from -190 to 190 ohms for each of the four loading configurations B,C,D and E. The results are plotted in terms of a span of the phase angle defined as a *delta phase angle*. This is simply the maximum continuous phase shifting capability of the antenna that can be expected within the -3dB limits of the forward gain of the antenna.

Results obtained are shown in Figure 10. The delta phase angle decreased from 33 to 20 to almost zero degrees when the second probe was stepped successively from positions B to C to D. The B and E configurations produce the same delta phase angle. However, the E loading configuration produces more cross-polarized radiated power than that of the B loading configuration. In fact, the results of the simulation predict that for configuration B, the cross polarized power is 0.00084% of the total power whereas for configuration E, the cross polarized power is 0.3% of the total power. Both are small, but configuration E produces 357 times as much cross polarized power as configuration B. Therefore the B configuration is the best choice for orientation of the probes in terms of reduction of unwanted cross polarized radiation. This leads us to conclude that the best performance in terms of maximum phase shift *and* minimal cross polarized radiation can be obtained by orienting the probes in the same direction as the electric field for the dominant TM01 mode of the antenna.

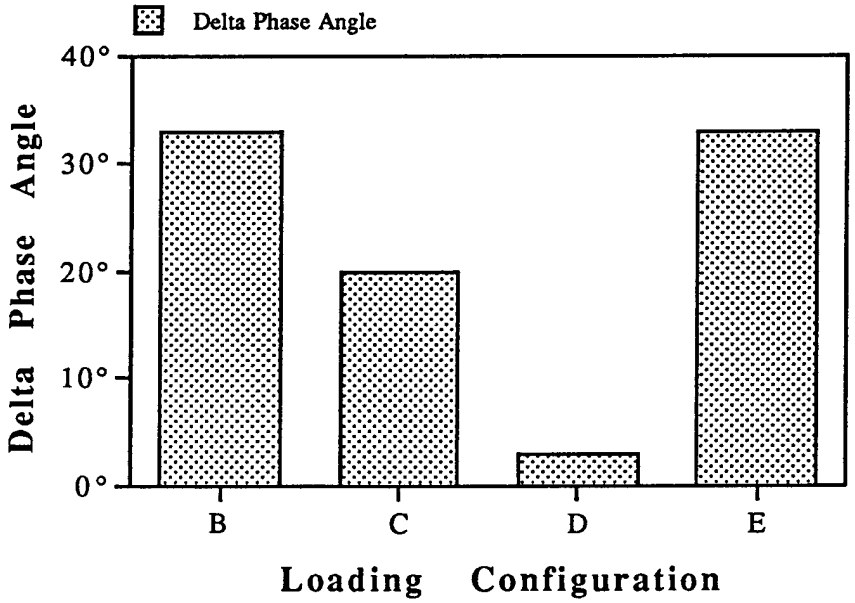

Figure 10. *Delta phase angle vs. loading configuration.*

The first objective of this study was to investigate the effect of the orientation of the probes in the dual probe loading configuration. Results shown in Figure 10 show that loading configuration B should be the candidate loading configuration. Logically, the next step in this investigation was to find the dual probe loading configuration that produced the maximum phase shift. To this end, two different dual probe

loading configurations were investigated. The first, shown in Figure 11, has one dual probe load and the second, shown in Figure 12, has two dual probe loads. The distance d between the probes for both configurations was varied uniformly from 0.024λ to 0.25λ in 0.024λ steps to determine the effect of spacing on the phase shifting ability of the antenna. Figure 13 compares the results of the two configurations and shows that a maximum phase shift of between 40 to 50 degrees of phase shift was possible with these loading configurations and positions on the patch. It also shows that generally speaking, the doubly loaded patch provides more phase shift than the singly loaded patch.

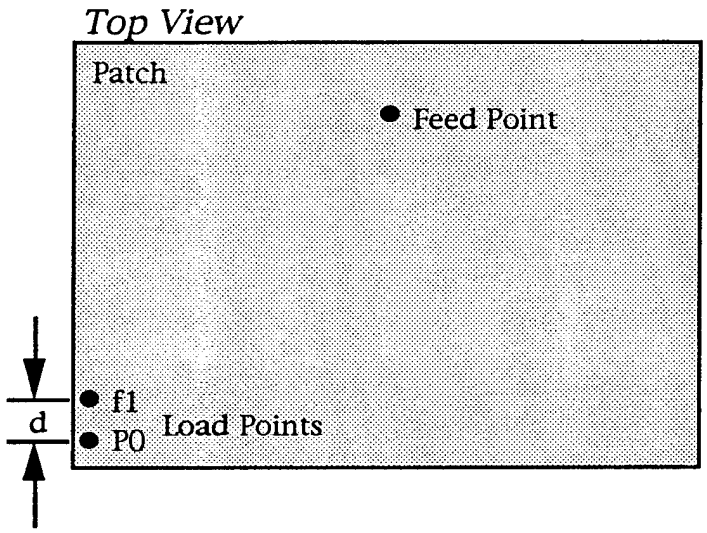

Figure 11. *Top view of patch with one dual probe load Separation distance d=0.024λ*

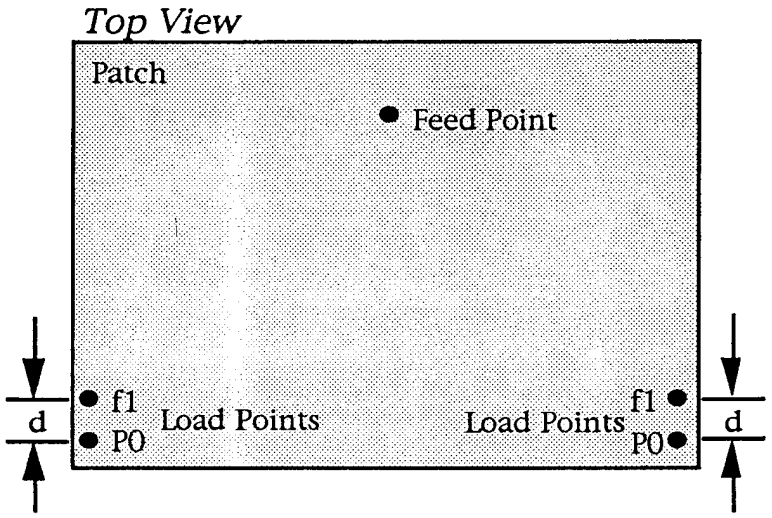

Figure 12. *Top view of patch with two dual probe loads Separation distance d=0.024λ*

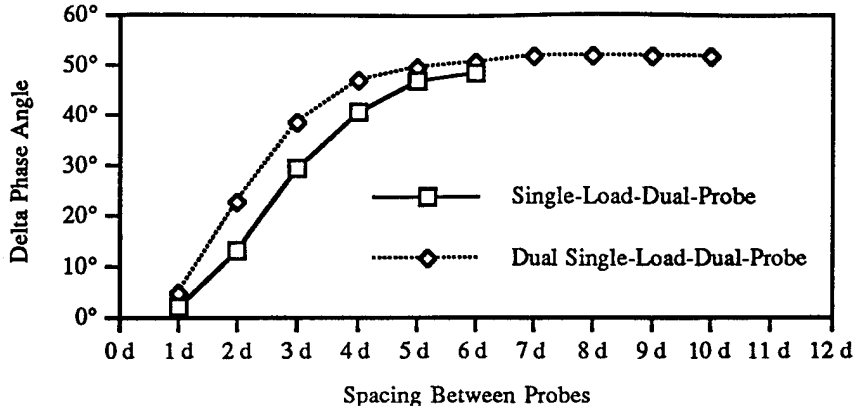

Figure 13. *Preliminary comparison of transmission phase shift of two different loading configurations vs. probe spacing Separation distance* $d = 0.024\lambda$

A further extension of the methodology used to investigate the doubly loaded element can be applied to multiple loads in a manner similar to that shown in Figure 11. We have proposed to investigate this multiple load configuration under a future research grant. From Figure 13, the two dual probe load configurations produce more delta phase angle than the one dual probe load configurations. These initial findings support our hypothesis regarding multiple control points.

Experimental Results

In addition to a number of computer simulations of the loaded microstrip antenna, several experiments were performed in an anechoic chamber. Various combinations of varactor diodes in series with surface mounted capacitors were placed on a rectangular element which resulted in varying amounts of S21 phase shift over the bias range of a given varactor. To date, between 45 and 55 degrees of phase shift have been observed with the antenna measured on boresight and the forward S21 transmitted power within the -3dB limits of the unbiased condition. That is, the received power was set to 0dB with no bias voltage and the frequency of the source adjusted for maximum received signal. Then phase measurements were taken as the varactor bias voltage was adjusted until the received power was -3dB. One particular measurement yielded about 75 degrees of phase shift, but the results of all measurements taken to date suggest that the 45 to 55 degree range mentioned above is consistently achievable with the *one particular loading arrangement* that has been investigated so far. This arrangement consisted of a Seimens BB811 varactor in series with a 10pF surface mounted capacitor. The series capacitor served as a DC blocking capacitor for bias isolation as well as to reduce the overall load capacitance of the capacitor/varactor combination. Since the capacitive reactance of any capacitor approaches minus infinity as the capacitance approaches zero, the slope of the reactance is very steep for very small capacitance values. Thus, it was hypothesized that as the overall capacitance became very small, the S21 phase change would be greatest for a given change in capacitance. Therefore, various capacitor values in series with the varactor were tried. A value of 10pF seemed to give the best results, although this was not the smallest series capacitor that was used. We have tried only a limited number of varactor diodes (Seimens) and it is possible that another manufacturer (such as Motorola) may have a line of diodes that may yield better results than those achieved so far. Also, only one load location has been tried so far; efforts were directed towards achieving repeatability since the baseline data was first obtained. Indeed, a technology is useless if it is not repeatable from one production run to the next. The baseline data was obtained from a rectangular element loaded with the loading combination described above and fed with a 2.3 GHz source. Data for three subsequent patches (labeled as 2nd, 3rd, and 4th elements) as well as the baseline data is shown on the following pages. The 2nd, 3rd & 4th patches were constructed to establish whether results obtained earlier could be repeated.

Figure 14 shows the baseline results obtained for this antenna. The -3dB point occurs at a bias voltage of around 19 volts and the corresponding phase shift is roughtly 45 degrees. The greatest rate of change of the S21 phase occurs at the minimum of the magnitude response.

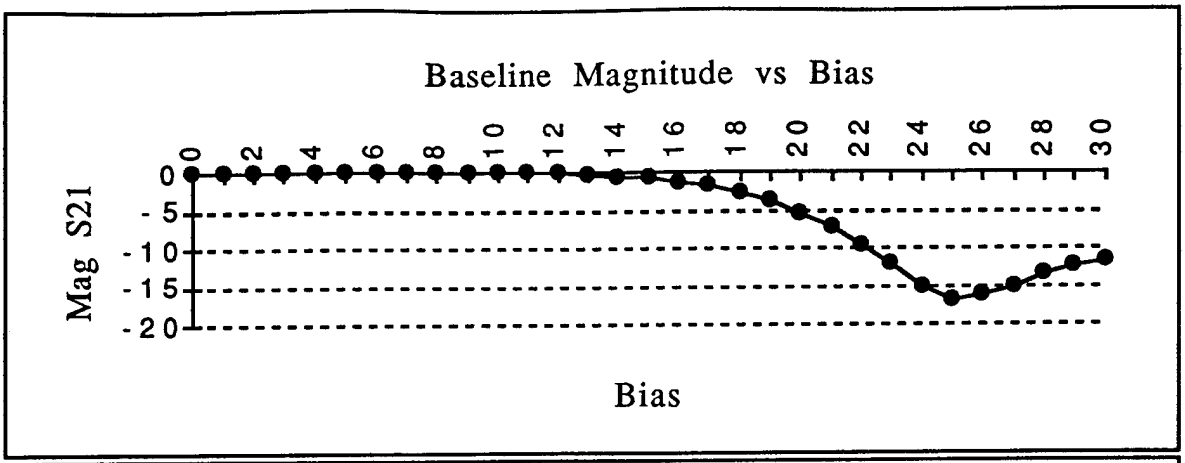

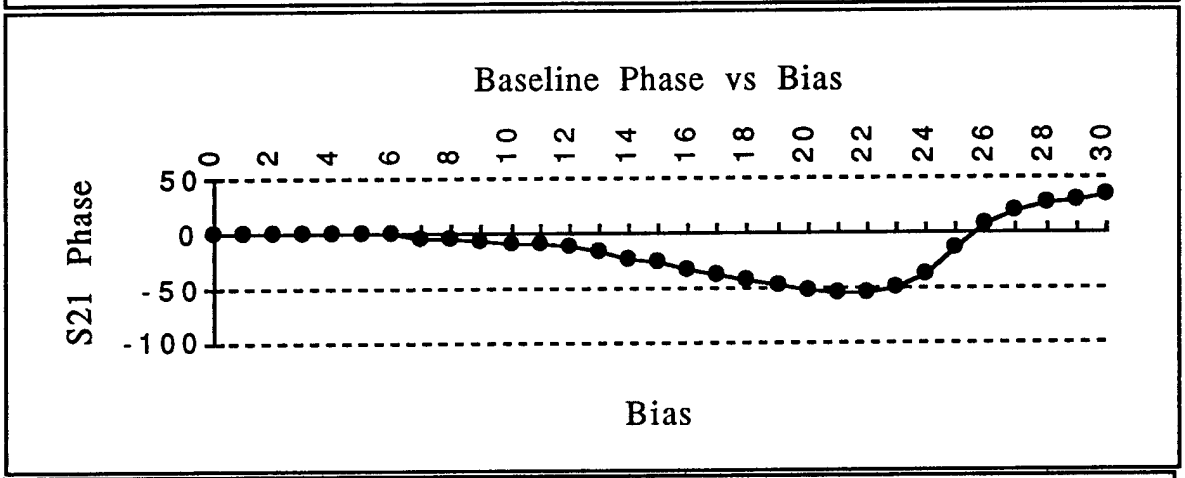

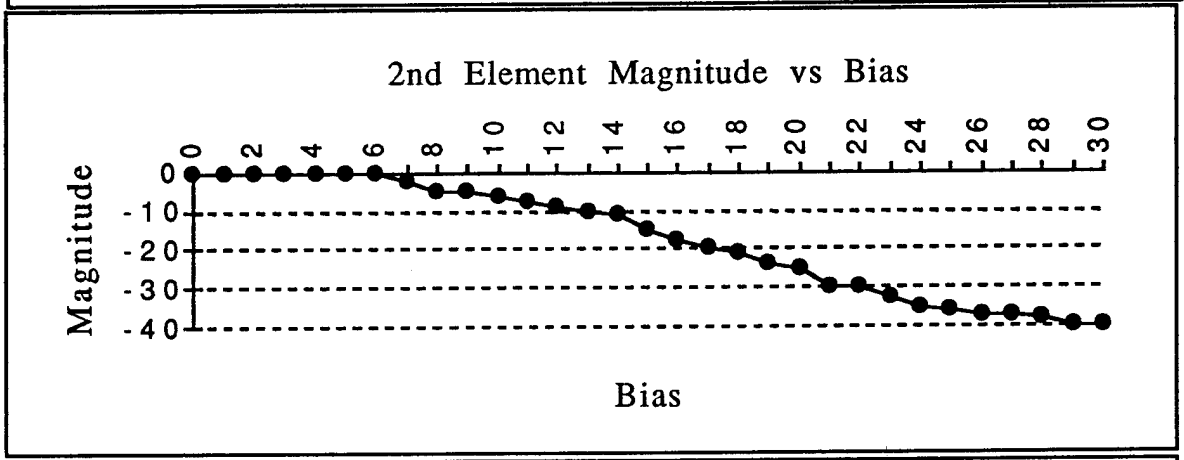

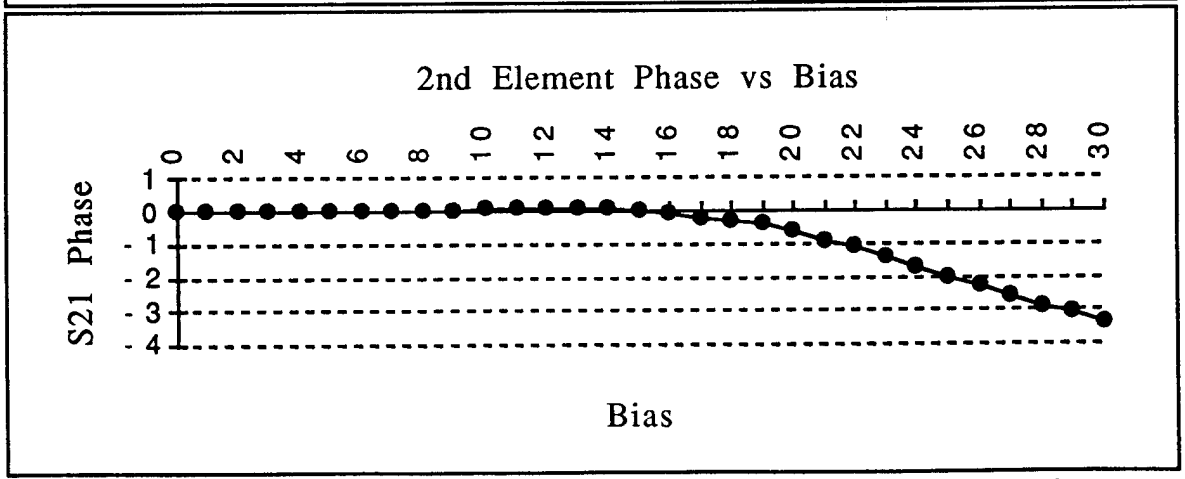

Figure 14. *Baseline & 2nd element magnitude & phase vs bias*

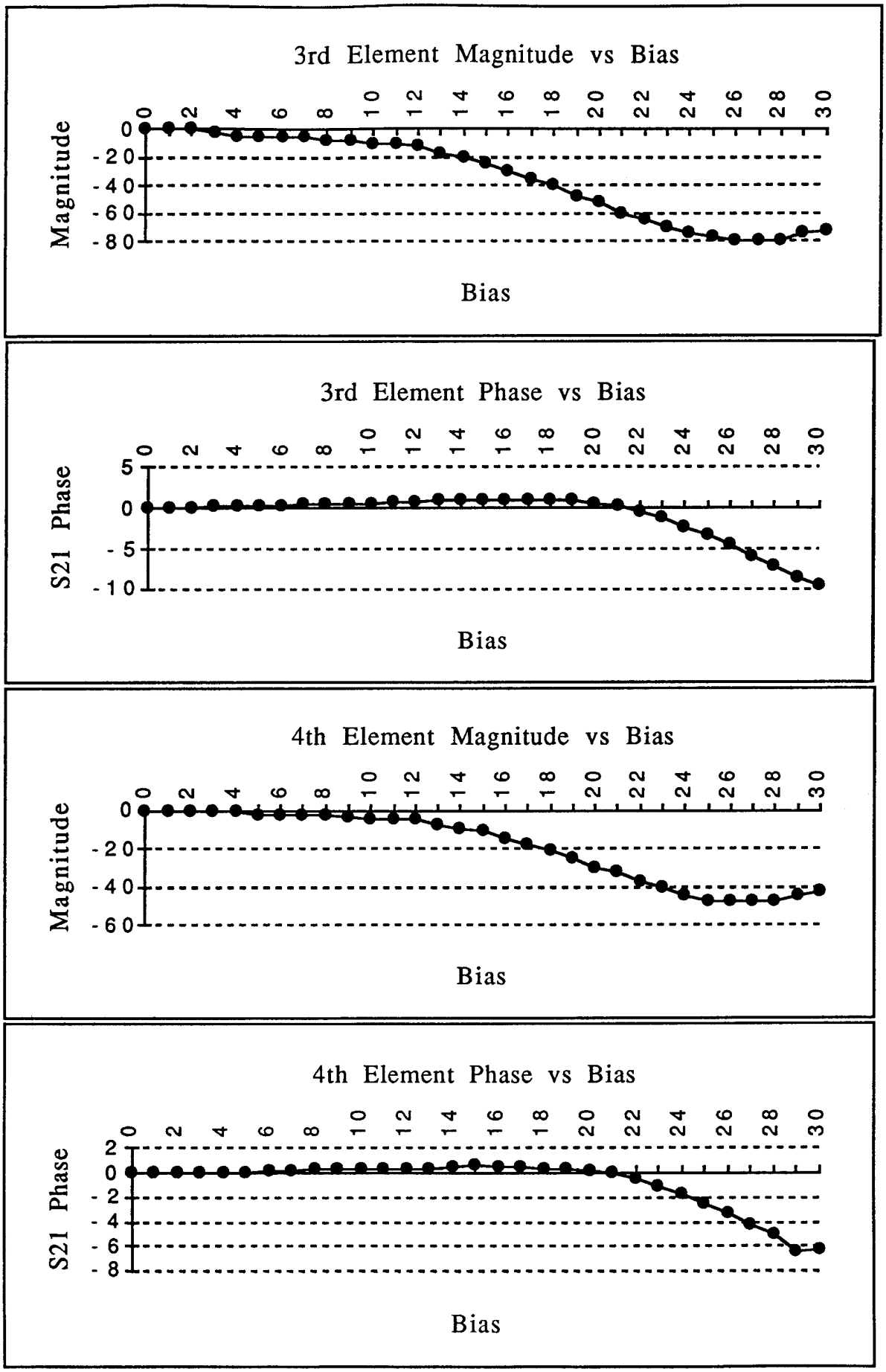

Figure 15. *3rd & 4th element magnitude & phase vs bias*

The following figures compare all 4 sets of data on common graphs.

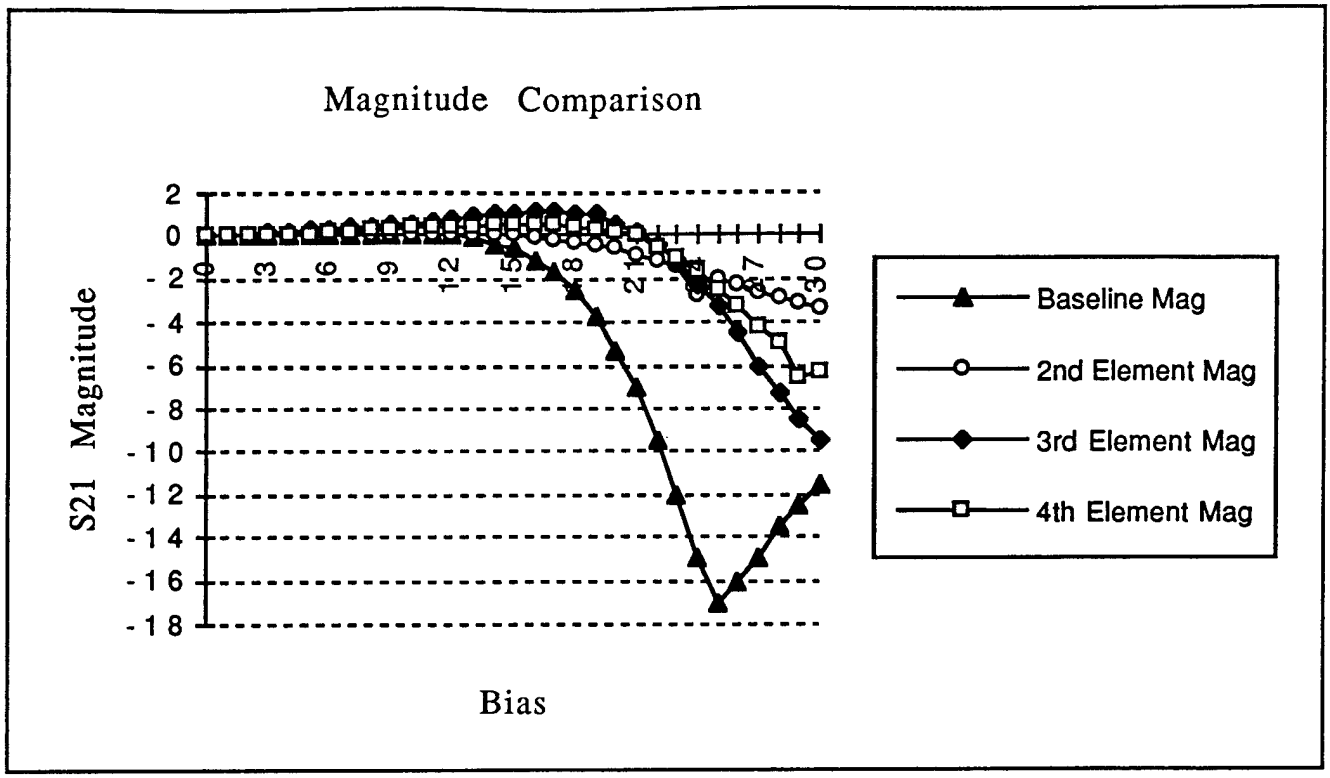

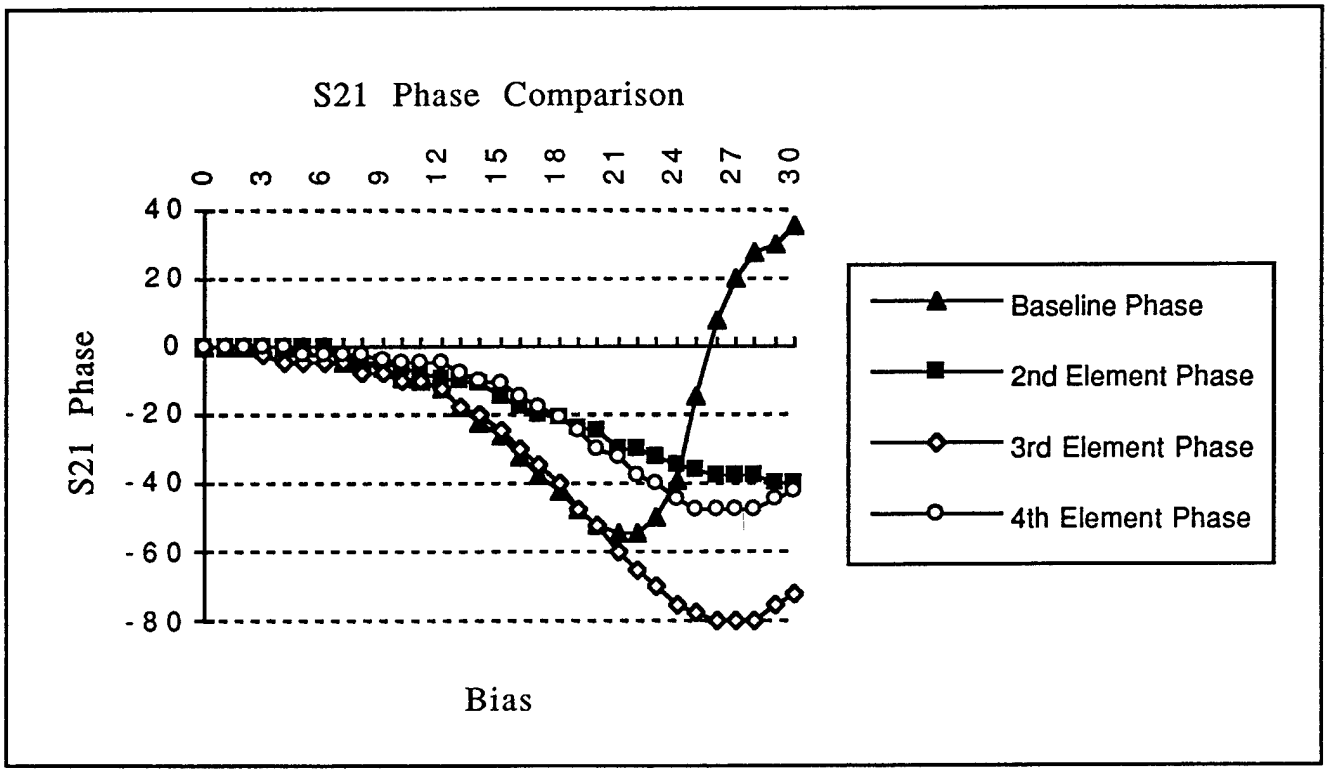

Figure 16. *Magnitude & phase comparisons*

By examining the magnitude responses in Figures 14 and 15, we can see that the responses of the 2nd, 3rd and 4th elements are similar while that of the baseline element deviates noticibly from the other three responses.

This is most likely due to a difference in thickness between the baseline element and the other three elements as well as differences in patch sizes which would have shifted the resonant frequency slightly. Also, load location may not have been identical in each antenna. Finally, since the antennas were not identical, the load (assuming the arrangements to be nearly identical) will have a different effect on the input impedance over the bias range of the diode. Thus, at around 25 volts, the baseline patch S21 forward gain is at a minimum (around -17dB) which is due to the impedance mismatch at the feed while the other three magnitude responses are on the order of about -3dB which means that the input impedance is significantly better matched to the source at this bias voltage. However, the three patches that were produced at the same time (2nd, 3rd & 4th elements) have fairly similar magnitude responses which indicates that the manufacturing differences do not have a drastic effect on the magnitude of the forward gain.

From Figure 16, the phase responses of the 2nd and 4th elements are close while those of the baseline element and the 3rd patch vary considerably. The 3rd element maximum phase shift is around 75 degrees while the 2nd & 4th patches yield around 40-50 degrees. The general shapes are very similar in that the greatest rate of phase change takes place when the magnitude response is at a minimum as can be seen from the baseline magnitude and phase responses. The shapes of the responses from the other three antennas seem to be the same, only shifted-to-the-right slightly. By examining the plots in Figure 16, it can be concluded that the phase response is a more sensitive function of manufacturing tolerances than the corresponding magnitude response in the region where the magnitude is less than -3dB down (i.e. where the magnitude is smaller). However, in the region where the magnitude is greater than -3dB (where the forward gain is larger) the responses are fairly well grouped. This is also encouraging in terms of repeatability since this is the useful operating region of the antenna.

Conclusions and Future Research

The results of this research have shown that between 45 and 55 degrees of phase shift can be attained experimentally with the loading arrangement and location that we have chosen. Simulation results have predicted about 30 to 40 degrees of phase shift for the same loading type (single load, single probe). The dual probe type of loading configuration has produced between 40 and 50 degrees of phase shift with the doubly loaded element generally yielding more phase shift over the range of probe spacings than the singly loaded element. Thus, it can be concluded from this research that the dual probe structure yields better results than the single probe structure and that two dual probe loads outperform one dual probe load. A natural inference is that multiple (more than two) dual probe loads will yield better results than the doubly loaded element. This is proposed

to be investigated in the future. It should also be mentioned that this type of loading structure offers more degrees of freedom than the single probe load. The single probe load can be varied in position only whereas the dual probe type of load can vary in position, radius, and orientation.

A sufficiently accurate model for the varactor diode is not yet available so that theoretical results from computer simulations and experimental results obtained from measurements cannot be compared directly. This is also one of the items proposed to be developed in future research on this project.

A great deal of experimental work will have to be performed to determine if a full 360 degrees of phase shift can be attained through the use of reactive loading. A very large number of simulations will have to be performed and a large number of experimental prototypes built before this determination can be made. An accurate varactor diode model for all values of bias voltage needs to be developed so that the repetitive burden of trying different loacations, etc. can be left largely to the computer. We have proposed to carry out these tasks in a further investigation of this phenomenon.

References

[1] D. D. Greig and H. F. Engleman, "*Microstrip - a new transmission technique for the kilomegacycle range*", Proc. IRE, vol. 40, pp. 1644-1650, 1952.

[2] G. A. Deschamps, "*Microstrip microwave antennas*", 3rd USAF Symp. on Antennas, 1953.

[3] E. J. Denlinger, "*Radiation from Microstrip Resonators*", IEEE Trans. on Microwave Theory and Techniques, pp 235-236, April 1969.

[4] J. Watkins, "*Circular Resonant Structures in Microstrip*", Electronics Letters, vol. 5 , no. 21, pp 524- 525, Oct. 1969.

[5] J. Q. Howell, "*Microstrip Antennas*", IEEE AP-S. Int. Symp. Digest, pp177-180, Dec. 1972.

[6] R.E. Munson, "*Conformal Microstrip Antennas and Microstrip Phased Arrays*" IEEE Trans. on Antennas and Propagation, pp. 74-78, Jan. 1974.

[7] A.G. Derneryd, "*Linearly Polarized Microstrip Antennas*", IEEE Trans. on Antennas and Propagation, PP. 846-851. Nov. 1976.

[8] D. H. Schaubert, F. G. Farrar, A. Sindoris, and S. T. Hayes, "Microstrip Antennas with Frequency Agility and Polarization Diversity", IEEE Trans. on Antennas and Propagation, vol. 29, no. 1, pp 118-123, Jan. 1981.

[9] Y.T. Lo, D. Solomon, W.F. Richards, "*Theory and Experiment on Microstrip Antennas*", IEEE Trans. on Antennas and Propagation, vol. 27, no. 2, pp 137-145, March 1979.

[10] W. F. Richards, Y.T. Lo, D. D.. Harrison,"An Improved Theory for Microstrip Antennas and Applications", IEEE Trans. on Antennas and Propagation, vol. 29, Jan. 1981.

[11] W. F. Richards, S. Davidson, S. A. Long, "*Dual-Band Reactively Loaded Microstrip Antenna*", IEEE Trans. on Antennas and Propagation, vol. 33, May 1985.

[12] W. F. Richards, Y. T. Lo, "*A Simple Theory for Reactively Loaded Microstrip Antennas*", IEEE AP Symp. pp 259-262, 1984.

[13] P. K. Agrawal, M. C. Bailey, "An Analysis Technique for Microstrip Antennas", IEEE Trans. on Antennas and Propagation, vol. 25, Nov. 1977.

[14] K. C. Gupta, "*Multiport-Network Modeling Approach for Computer-Aided Design of Microstrip Patches and Arrays*", IEEE AP-S International Symp., June 1987.

[15] A. Benalla and K. C. Gupta, "*Multiport Network Model and Transmission Characteristics of Two-Port Rectangular Microstrip Patch Antennas*", IEEE Trans. on Antennas and Propagation, vol. 36, no. 10, Oct. 1988

[16] A. Benalla and K. C. Gupta, "*Multiport Network Approach for Modeling the Mutual Coupling Effects in Microstrip Patch Antennas and Arrays*", IEEE Trans. on Antennas and Propagation, vol. 37, no. 2, Feb. 1989.

[17] P. Bhartia and I. J. Bahl, "*Frequency Agile Microstrip Antennas*", Microwave Journal, pp. 67-70, Oct. 1982.

[18] M. H. Thursby, B. Grossman, K. Yoo, "*Neural Networks and the Control of Smart Systems*", United States Army Research Office Workshop, Smart/Intelligence Materials & Systems, March 19-23 1990.

[19] J. T. Aberle, M. Chu, and C. R. Birtcher, "*Scattering and Radiation Properties of Varactor-Tuned Microstrip Antennas*", IEEE AP-S. Symp. Digest, pp. 2229-2232, 1992.

[20] R. B. Waterhouse and N. V. Shuley, "*Frequency Agile Microstrip Rectangular Patches Using Varactor Diodes*", IEEE AP-S. Symp. Digest, pp. 2188-2191, 1992.

[21] E.H. Newman, P. Tulyathan, "*Analysis of Microstrip Antennas Using Moment Methods*", IEEE Trans. on Antennas and Propagation, vol. 29, pp. 47-53, Jan. 1981.

[22] D. M. Pozar, "*Input Impedance and Mutual Coupling of Rectangular Microstrip Antennas*", IEEE Trans. on Antennas and Propagation, vol. 30, no. 6, pp. 1191-1196, Nov. 1982.

[23] J. T. Aberle and D. M. Pozar, "*Accurate and Versatile Solutions for Probe-Fed Microstrip Patch Antennas and Arrays*", Electromagnetics, vol. 11, no. 1 , pp. 1-19, 1991.

[24] M. H. Thursby, R. M. Hsu, "*Phase Control of a Micropatch Antenna Element*", SPIE Proceedings of Smart Structure and Intelligent Systems, SPIE vol. 2190, pp. 476-483, Feb. 1994.

[25] M. H. Thursby, K. Yoo, B. Grossman, "*Neural Control of Smart Electromagnetic Structures*", accepted for publication by IEEE Trans. on Aerospace and Electronics Systems, 1994.

[26] K. Yoo, "*Robust Control of a Linear System with Plant Uncertainties Using an Artificial Neural Network*", Ph.D. Dissertation, Department of Electrical and Computer Engineering, Florida Institute of Technology, June 1993.

[27] J. R. James and P. S. Hall, "*Handbook of Microstrip Antennas*", IEE Electromagnetic Waves Series 28, vol.1 & 2, published by Peter Peregrinus Ltd., London, United Kingdom, 1989.

[28] R. M. Hsu and M. H. Thursby, "*Phase Control of a Micropatch Antenna Element Designed for Monolithic Phased Arrays,*" IEEE MTT-S Digest Vol. 3, pp 1507-1510. 1995